Chapter 5

Fast Timing System

5.1 Introduction

Overlap background due to multiple proton-proton interactions in the same bunch crossing will become prevalent at the LHC as the instantaneous luminosity increases. Much of this background can be removed by kinematical matching between the central system as measured by the central detector (for example, jets from Higgs decay), and inferred from the protons measured in the AFP silicon detectors. For rare processes, the background may still be too large to make a significant measurement, motivating the fast time-of-flight detector. Consider an event with a central massive system and two oppositely directed small angle protons. If the protons are from the same interaction as the central system, the position of the vertex as measured by the central tracks will be consistent with the position as determined from the time difference of the outgoing protons. A time resolution of 10 ps corresponds to a 2.1 mm vertex position resolution, which given the approximately 5 cm width of the luminous region and the 50 μm uncertainty of the central vertex will yield an additional rejection factor of about 20 against this fake background.

5.2 Timing system requirements

The final timing system should have the following characteristics

- 10 ps or better resolution
- acceptance that fully covers the proton tracking detectors
- efficiency near 100%
- high rate capability (O(10) MHz/pixel)
- segmentation for multi-proton timing
- Level 1 trigger capability
- radiation tolerant
- robust and reliable

For the first stage, 220 m at modest luminosity, the requirements are not quite as stringent: 20 ps resolution will suffice, the rate should not exceed 2 MHz/pixel, and the Level 1 trigger capability is not strictly necessary.

Another important aspect for this system is its stability and monitoring. For this reason, we are planning to add an ADC to measure the pulse height, which would allow us to monitor any PMT aging effects and also to perform a residual time walk correction. In addition, we are adding a fiber pulser system which will also allow us to monitor the whole electronics chain. Finally, we will collect samples of hard diffractive events with two protons and two central jets that can be used to monitor the stability of the z-vertex position.

Since the driver for the highest precision of timing is pileup at the highest luminosity levels, especially for light resonances, it is clear that 20 or 30 ps is adequate for the first stage when we only have 220 detectors. We will, of course, have the best possible resolution for 220 m that we can obtain in 2013: we believe this will be ∼10 ps. It is likely that parts of the system would be upgraded in a 420 m stage leading to better timing resolution.

5.3 Timing system components

The main components of the timing system are: i) the detector comprised of the radiator that produces light when a proton passes through it and the photo-sensitive device that converts the photons into an electrical pulse; ii) the electronics system that reads out the pulse and interfaces with the ATLAS data acquisition and trigger system; and iii) the reference timing system that provides a low jitter clock signal allowing the correlation of the detector stations which are hundreds of metres apart. Below we describe each of these components.

5.3.1 The detectors

Typically high energy physics time-of-flight detectors have a resolution of about 100 ps [48], an order of magnitude worse than our requirements. Recently spurred by a sub-10 ps measurement obtained in Ref. [49], the focus for dramatically improving time-of-flight resolution has turned towards detectors employing a quartz Cerenkov radiator coupled with a microchannel plate photomultipier tube (MCP-PMT).

We note that the detector design of Ref. [49] does not suit our needs, since it requires putting the MCP-PMT directly in the beam. Over the past several years, we have studied Cerenkov detectors with gas (GASTOF) and quartz (QUARTIC) radiators [50, 24, 1]. Cerenkov radiation is emitted along a cone with an angle defined by the Cerenkov angle $\theta_c \approx \cos^{-1}(1/n)$, where n is the index of refraction of the radiator.

Figure 5.1(a) shows a schematic diagram of the QUARTIC detector, which consists of four rows of eight 5 mm × 5 mm quartz or fused silica bars ranging in length from about 8 to 12 cm and oriented at the average Cerenkov angle (∼ 48° for quartz). Photons are continuously emitted as the proton passes through the bars; those emitted in the appropriate azimuthal angular range are channeled to the MCP-PMT. Any proton that is sufficiently deflected from the beam axis will pass through one of the rows of eight bars, providing, in principle, eight independent time measurements along the track, and an overall resolution that is $\sqrt{(8)}$ smaller than the single bar resolution of 30 ps. Our studies have shown that there are various cross talk effects that correlate the measurements, dominated by optical and charge sharing between neighboring channels. Due to the isochronous detector design, however, the cross talk signal is approximately in-time, as a result we do observe the $\sqrt{(n)}$ scaling of the single bar resolution.

Figure 5.1(b) shows a schematic diagram of the GASTOF detector. It has a gas radiator

at 1.3 bar in a rectangular box of 20 to 30 cm length, with a very thin wall adjacent to the Hamburg pipe pocket. The protons are all essentially parallel to the axis. A thin 45° concave mirror at the back reflects the light to an MCP-PMT. The gas used in tests is C_4F_8O, which is non-toxic and non-flammable, and has a refractive index of $n = 1.0014$ giving a Čerenkov angle ($\beta = 1$) of 3.0°.

Figure 5.1(c) shows a schematic of an MCP-PMT which consists primarily of a photocathode and microchannel plates. The photo-cathode converts the radiation to electrons, and the MCP's, which are lead glass structures with an array of 3 to 25 micron diameter holes (pores), serve as miniature electron multipliers converting the incoming photons to a measurable signal for the downstream electronics. Phototubes under consideration for QUARTIC Stage 1 are the Photonis Planacon a 64 channel 2 inch square tube with either 10 or 25 μm pores, or the Hamamatsu SL10 a 16 channel 1 inch square tube with 10 μm pores, while a Photek 210 single channel 1 cm tube with 3 μm pores or a Hamamatsu R3809U-50 with 6 μm pores are the leading candidates for GASTOF.

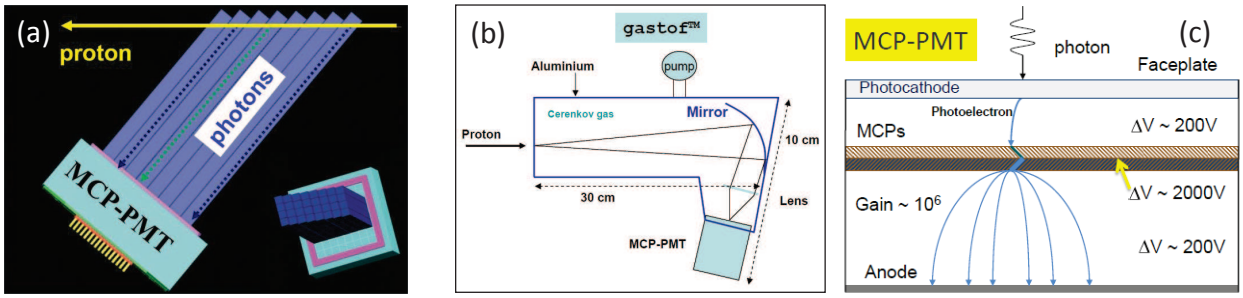

Figure 5.1: (a) A schematic side view of the proposed QUARTIC time-of-flight counter, which shows Cerenkov photons being emitted and channeled to the MCP-PMT as the proton traverses the eight fused silica bars in one row. The inset shows a rotated view with all four rows visible. (b) A schematic view of the proposed GASTOF time-of-flight counter. (c) A schematic view of an MCP-PMT as described in the text.

The AFP R&D effort has focussed on the QUARTIC detector, which is segmented and thus meets the requirements of Sec. 5.2 better than the GASTOF detector. The QUARTIC longitudinal segmentation provides multiple measurements of the same proton, reducing the necessary precision for any single measurement to 30 to 40 ps, while the transverse segmentation provides the ability to measure multiple protons in the same detector. It is also useful to have a GASTOF, however, since it makes one excellent measurement (better than 20 ps), providing a useful cross check for QUARTIC.

5.3.2 The electronics

The electronics system is designed to provide a 20 ps or better resolution measurement of the time-of-flight of protons scattered at small angles, provide a Level 1 trigger, and record the time measurements in the ATLAS data stream. The electronics are optimized for the QUARTIC detector, which makes multiple measurements in the 30 ps range, but can also be used for GASTOF, which makes a single measurement in the 10 to 20 ps range. Figure 5.2 presents a schematic overview of the electronics system and includes photos of the primary constituents: pre-amplifiers, constant fraction discriminators, trigger, and high precision time-to-digital converters (HPTDC). The reference timing system, which provides a stable clock signal, is described in Sec. 5.3.3.

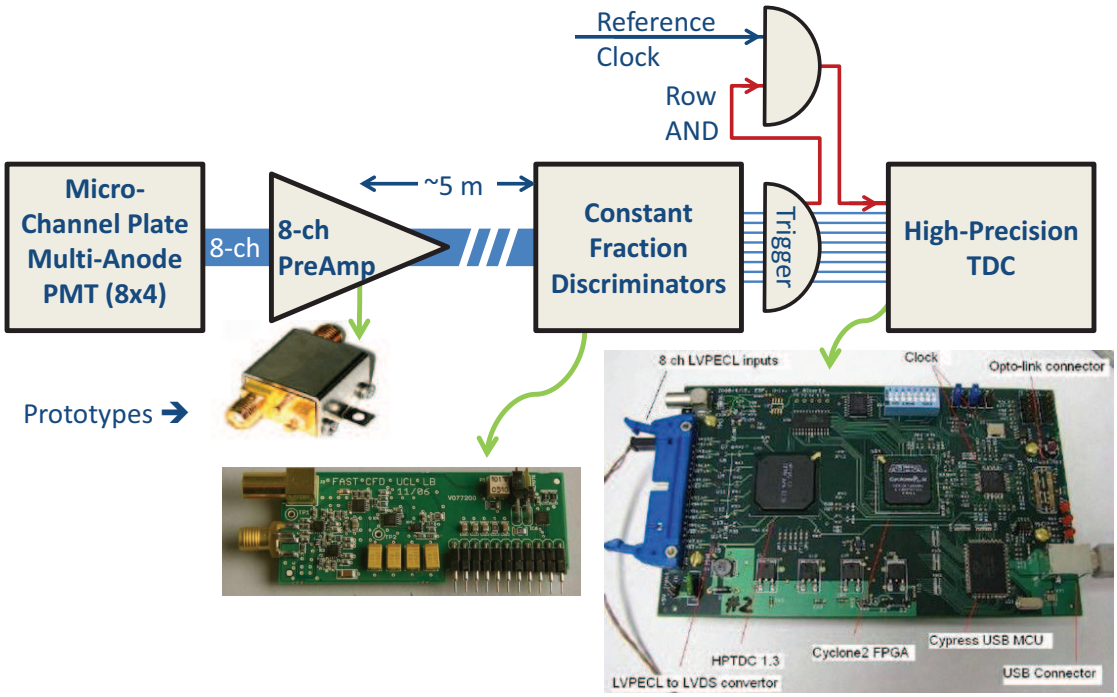

Figure 5.2: A schematic diagram of the electronics chain described in the text. The photographs show a low noise Minicircuits ZX60 pre-amplifier, a constant fraction discriminator daughter board, and the HPTDC board used in laser and beam tests.

Pre-amplification. Given proton rates on the MHz level, the MCP-PMT gain should be as low as possible to maximize the device lifetime and minimize the saturation of the pores. We have determined that a $\times 50$ pre-amplification allows us to run the Burle Planacon tube at low gain, while still yielding the several hundred mV signals required for optimal timing performance. In Sec. 5.5 we show that for multiple photoelectrons one can run at lower gain without compromising the timing resolution. The exact gain factor required depends on the final choice of the MCP-PMT. Tests have been performed using two $\times 10$ Minicircuits 8 GHz ZX60 amplifiers in series, separated by a $\times 2$ attenuator and a diode to protect the second amplifier from large signals in the case of shower events. Although a bandwidth of 1–2 GHz would suffice for a typical multi-anode MCP-PMT (with a rise time of about 400 ps), we did not find an amplifier in this bandwidth range that had the desired gain as well as low noise (1 dBm) and reasonable cost ($50 per channel). For the final detector electronics we will replace the ZX60 with a 3mm $\times$ 3mm Minicircuits QFN low profile surface mount pre-amp, and incorporate this and the other discrete components on a PCB board that will plug directly onto the MCP-PMT.

Constant fraction discriminator. The amplified signals will then be sent via $\sim$30 metre long high speed coax cables to the constant fraction discriminator (CFD) boards located in a readout crate in the alcove at 240 m. Preliminary tests indicate that a several meter cable run does not introduce significant jitter (recall a single measurement requires a precision of "only" about 30 ps). Tests of the signal integrity with the final cable type and distance will be performed soon. The CFD system is based on a design developed by the University of Louvain for FP420 [24] with a NIM unit mother board that filters the NIM power and houses 8 single channel CFD daughter boards. These provide a NIM output for testing and an LVPECL output to the HPTDC board that digitizes the time. The final system may be VME based instead of NIM, and will also form a trigger signal prior to being digitized.

Trigger. A coincidence of several CFD channels in the same row can be used to form a trigger. The row triggers can be ORed to form a global trigger that can be sent to Level 1 on a dedicated large diameter air core cable. This global trigger would be satisfied when a proton passes anywhere through the detector. A more sophisticated trigger could be formed in a second Stage of AFP after the L1 Calorimeter upgrade, by correlating the row trigger with the calorimeter η to chose events in a specific mass range. In addition to providing a global trigger, the row triggers can be used to limit the occupancy of the HPTDC board by only passing on the CFD signals for events that pass a multiplicity cut within a row. These row triggers will also be used to filter the reference clock signal, such that the clock signals are only passed to the associated HPTDC chips when the row in question has a proton passing through it.

The trigger circuit is still in the conceptual design stage. We plan to implement a simple resistive sum of digital CFD signals (or fractions thereof) and input this signal into a fast comparator to provide a multiplicity trigger. The ADCMP582 used in the current Alberta CFD is the leading candidate for this tas: it has a 200 fs random jitter and 180 ps propagation delay. The CFD signals must be delayed by this amount (cable delay) and then be gated. The gate will either be built from discrete components or with LVPECL chips and should have small transit time and jitter. The random jitter of the output drivers (SY58601 Micrel.com) in the current Alberta CFD is less than 1 ps and a typical transit time is 125 ps; other Micrel components, like their gates, have the same specification on random jitter and transit times less than 200 ps. Recall that an individual QUARTIC measurement is on the 30 ps scale, consequently jitter of a few picoseconds in the trigger circuit would not impact the overall system jitter.

HPTDC board The filtered CFD and clock LVPECL signals are sent to the HPTDC board via ribbon cable. This board uses the 25 ps least bit 8-channel HPTDC chip developed by CERN for the ALICE Time-of-Flight detector [51]. Our HPTDC board also includes control signals

and an optomodule which interfaces to the existing ATLAS Readout Driver (ROD). Our studies indicate that if operated in the standard 8-channel high resolution mode (25 ps least bit), the occupancy of the HPTDC board will eventually exceed 2 MHz causing a loss of data. Simulations show that by doubling the internal clock speed to 80 MHz and using only four channels per chip, the occupancy limit can be increased to 16 MHz at less than 0.1% losses. This capability is satisfactory for our expected maximum 10 MHz trigger rate, and using the filtering described above will also reduce the rate of the reference timing signal to acceptable levels.

5.3.3 Reference clock

The final component of the time-of-flight system is the reference clock used to tie together measurements hundreds of metres apart. Practically, this is done by taking the time difference with respect to a stabilized clock signal. For the clock signal to cancel in the time difference it must have a jitter of 5 ps or less, or it would not be negligible relative to the proton time resolution. The reference timing stabilization circuit is based on a design developed at the Stanford Linear Accelerator Center (SLAC) by Joe Frisch and Jeff Gronberg (LLNL). It uses a phase locked loop (PLL) feedback mechanism as shown in Fig. 5.3(a). A voltage controlled oscillator (VCO) launches a signal down the cable from the tunnel near the proton detector to the interaction point (IP), where it is reflected and sent back. At the IP end of the cable the signal is sampled with a directional coupler where it is compared in the mixer with the 400 MHz Master Reference, provided in this example from the LHC RF signal. The result is a DC voltage level that is fed back to the VCO to maintain synchronization. Changes in the cable's electrical length cancel when the original and returned signal are added. A high quality large diameter air core coaxial cable was used with a 476 MHz RF signal for preliminary tests (the LHC RF is 400 MHz, so minor modifications are needed to adapt the SLAC design), and the stabilization circuit yielded a 150 fs jitter over a 100 m cable. Figure 5.3(b) shows results from a second test, with a 300 m cable, which was left outside to verify the temperature stability of the circuit. A low noise amplifier was used to boost the return signal to recover the cable and power coupling losses, which are a function of cable length (the measured attenuation was about 7.5 dB for the 300 m cable). The unstabilized circuit was observed to have a variation of 80 ps/10 degrees C, while the stabilized circuit (shown in the figure) reduced the variation to 4 ps/10 degrees C. Given that the ambient temperature in the tunnel is stable within a degree or two, the effect of temperature drift is less than one picosecond.

The stabilized 400 MHz RF wave will then be converted to a 40 MHZ square wave that will provide an input signal to the trigger board, such that the clock will be provided to the HPTDC only for triggered events. This is necessary to keep the HPTDC occupancy below 15 MHz.

The PLL does need a 400 MHz signal, and we can generate our own signal if not available, since it is just a time stamp and is not associated with the scattering. We stabilize this generic 400 MHz signal to within a picosecond, and in the tunnel we convert this to a stabilized 40 MHz signal that we write out with the timing data.

Although this stabilized clock signal can drift with respect to the beam, this is not an issue since this drift will be identical for both sides and will cancel in the time difference. We will use double pomeron dijet events, which will provide both central vertices and correlated protons to calibrate the central vertex and the timing vertex, and monitor the stability of the reference system.

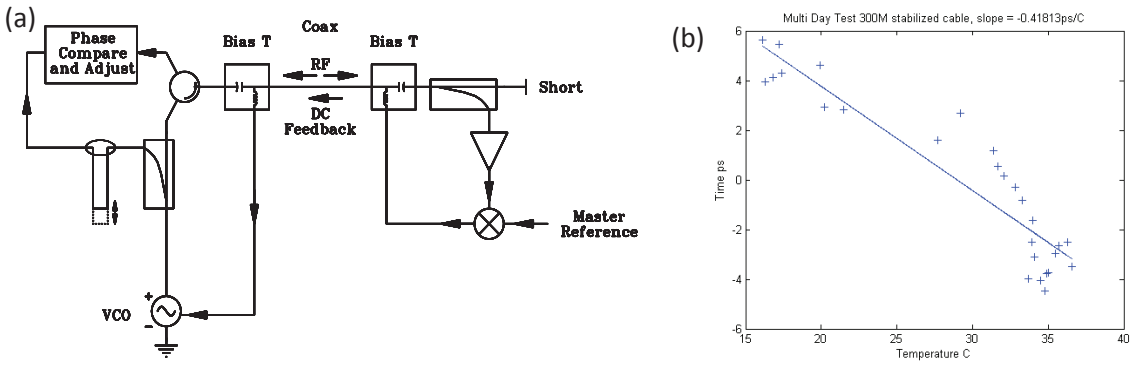

Figure 5.3: (a) Schematic of the Reference timing system as described in text.(b) Results of temperature stabilization test showing a mild drift with temperature (about 4 ps for 10 degrees C).

5.4 Timing system equipment

The Stage I timing system will consist of two to four 32 channel QUARTIC detectors, one or two on each side, with a channel count of 64 to 128. Each detector would be readout by one Photonis Planacon or two Hamamatsu SL10 MCP-PMTs. The natural unit of the electronics is eight channels based on the number of pixels in each row of the Planacon, so we will need 16 amplifier boards, trigger boards, and HPTDC boards for the four detector option. Including the possibility of a two-channel GASTOF detector for each side and two spares, brings the quantity of electronics boards to 20. The infrastructure will consist of high voltage for the MCP-PMT's (CAEN 1491 or similar, one module required per side plus a spare), low voltage for the amplifiers (12 V filtered), five VME crates (two per side plus a spare), and cables. The reference timing system will consist of two transmitter boxes, two receiver boxes, and one 300 m high quality cables per side. Including a Level 1 trigger cable and a spare for each side brings the total to six high quality cables.

5.5 Timing system performance

We have extensively studied the proposed QUARTIC detector, using simulations, beam tests, and laser tests. Figure 5.4 (reprinted from the Letter of Intent) shows data from a 2008 CERN test beam run with (a) the time difference between between two 90 mm long QUARTIC bars interfaced to a Photonis Planacon with 10 μm pores and read out by the constant fraction discriminator described above, and (b) the efficiency across the width of a bar. The time difference has an rms of about 56 ps, corresponding to 40 ps per bar (assuming the bars are equivalent and uncorrelated), while the efficiency is seen to be uniformly greater than 95% across the bar. The test beam data are consistent with 10 to 15 detected photoelectrons per bar confirming expectations from detector simulations.

Since the 2008 test beam most of the performance testing has been using a pulsed 405 nm laser at the UTA Picosecond Test facility. In this setup we replace the light from the detector with light from the laser, allowing us to explore in a controlled environment all aspects of the system from the MCP-PMT through the electronics. We have obtained a CFD resolution of better than 5 ps, assuming that the pulse is sufficiently amplified (typically we amplify the pulse to ensure an average pulse height of about 500 mV; pulses above 250 mV have very little

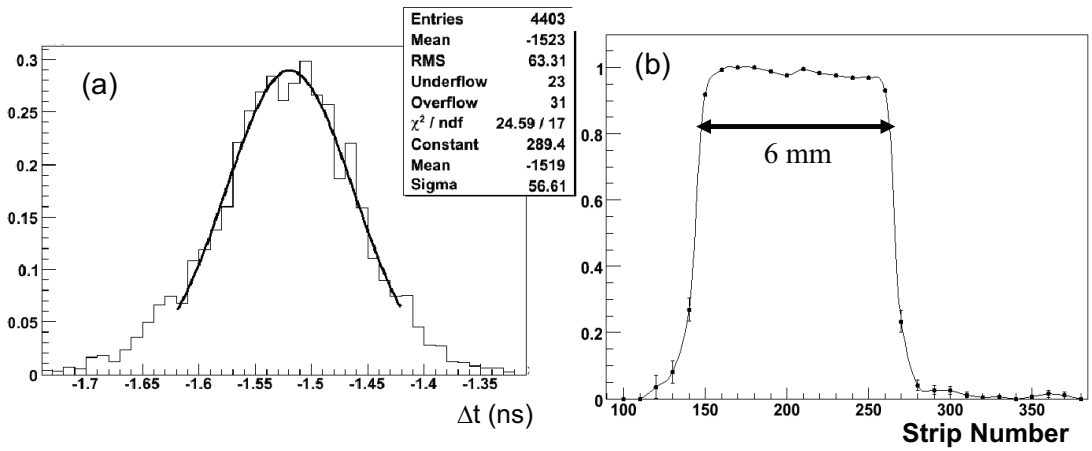

Figure 5.4: (a) The time difference between two 90 mm long QUARTIC bars described in text. (b) the fraction of track events that have a valid time in a QUARTIC bar, as a function of silicon strip number.

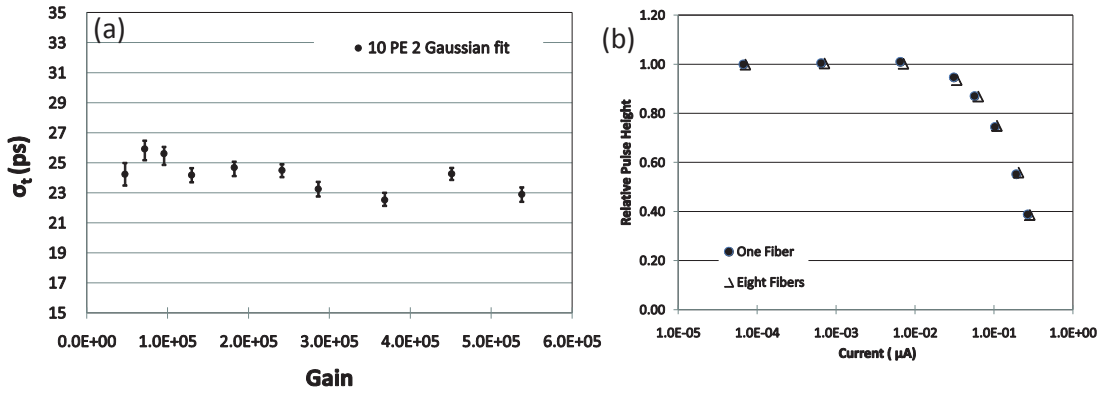

Figure 5.5: (a) Timing resolution versus gain and (b) the relative gain versus current (solid circles with one pixel hit in a row of eight and open triangles when all eight pixels hit in a row)for the 64 channel 10 μm Photonis Planacon tube.

residual timing dependence on pulse height after using the CFD). We have obtained an HPTDC resolution of about 14 ps, consistent with pulser tests done at Alberta. The 15 ps overall contribution from the CFD/HPTDC is quite acceptable given our overall goal of 30 ps/channel.

Figure 5.5(a) shows a key result from the laser tests, namely that the timing for the 10 μm pore 64 channel Photonis Planacon tube has very little gain dependence for gains as low as 5×10^4. This result is obtained for a laser setting with 10 pe's, the working point of the QUARTIC detector. The validation of low gain running is important as the main technical issues regarding MCP-PMTs are rate and lifetime concerns, both of which are reduced by a factor 20 compared to operation at the canonical 10^6 gain.

Figure 5.5(b) shows the relative gain as a function of calculated output current for our working point. We note for a laser frequency of 5 MHz (last point), corresponding to a calculated current of about 0.4 μA over a 0.2 cm^2 pixel, there is about a 60% gain reduction due to saturation of the pores which have a 1 ms recovery time. For the two previous points, corresponding to the expected maximum rates for Stage 1 of 1 to 2 MHz, the gain is only reduced by 20 to 40%. If

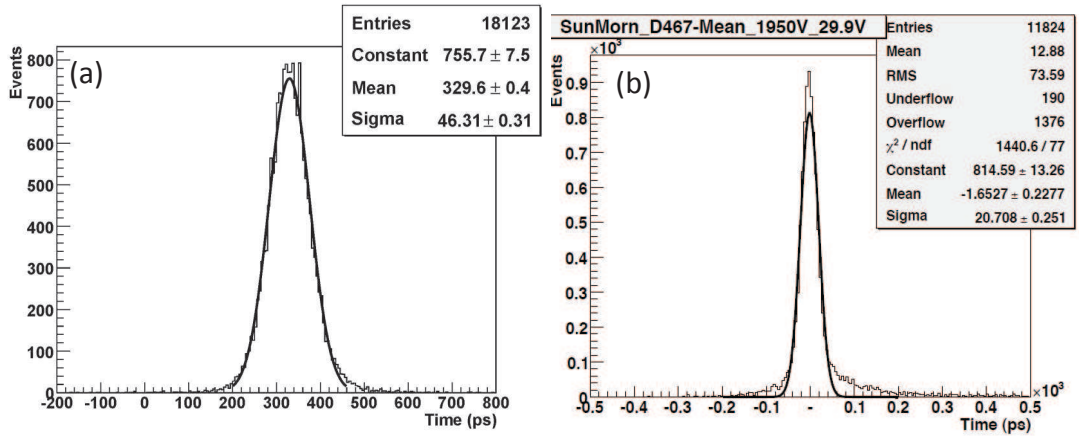

Figure 5.6: Results from November 2010 Fermilab test beam showing (a) the time difference between the CFD signal from two non-adjacent QUARTIC bars (bar 4 and 6) using the LeCroy 8620a oscilloscope (b) the time difference between a reference detector and the average time of three of the QUARTIC bars.

the amplification is augmented sufficiently, the timing resolution is observed to be independent of this saturation. This is within a factor of 10 of our expected maximum rate, and this final factor can be attained with a high current version of the Photonis tube already developed, thus meeting our maximum rate needs. We also note that this single channel result (closed circles) is unchanged when fibers are plugged into all eight pixels in a row (open triangles). demonstrating that saturation is a local effect.

More recent test beam data (Fermilab November 2010) using a better constructed single row prototype detector with a 25 μm Planacon yield better results. Figure 5.6 (a) shows the time difference as measured with a LeCroy 8620a oscilloscope of the CFD pulse from two non-adjacent bars. Although this MCP-PMT has inferior intrinsic time resolution due to the larger pore size (versus the 10 μm PMT, this is more than compensated for by the higher light yield (about 15 photoelectrons per bar) due to a higher quantum efficiency and a better constructed detector. The 46 ps width implies a single bar resolution of 33 ps including the CFD. Non-adjacent bars were chosen to minimize the correlation between channels. Figure 5.6(b) shows the time difference between a reference signal and the average time from three quartz bars. The reference signal is obtained using a quartz bar interfaced with a silicon photomultiplier (estimated to have 25 photoelectrons and a resolution of 13 to 15 ps). Taking into account the resolution of the reference signal, the 20 ps overall resolution implies that the three bar system resolution is about 15 ps (note this does not include the HPTDC resolution). Including HPTDC resolution we obtain better than 20 ps with 100% efficiency for a single 8 channel detector.

Figure 5.7 shows the time difference between two GASTOF detectors from a 2010 CERN test beam run, with $\delta t = 14$ ps (r.m.s.) implying a single detector resolution of 10 ps (measured with oscilloscope). Including the HPTDC resolution is expected to result in a better than 20 ps measurement, with some inefficiency.

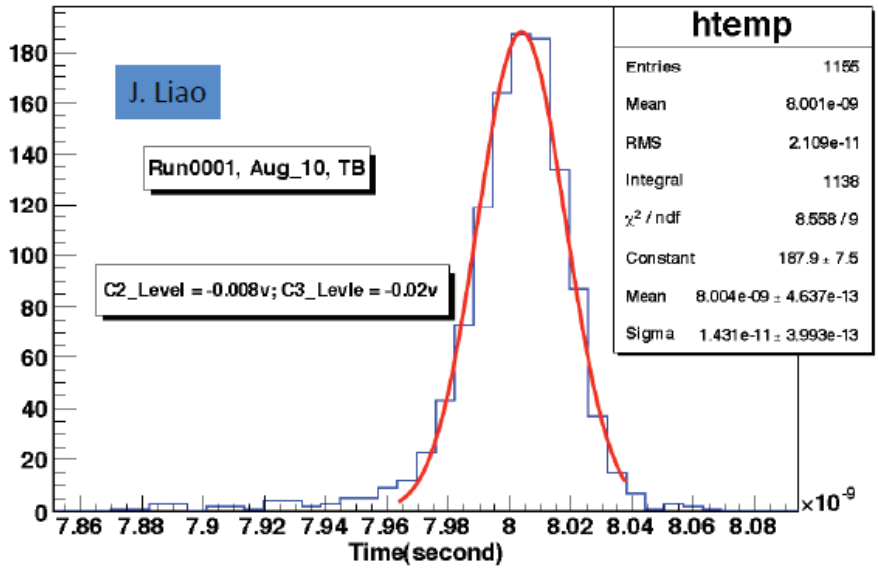

Figure 5.7: The time difference between two GASTOF detectors as described in text.

5.6 Ongoing research and development

We have developed a proof-of-concept of the fast timing detector system demonstrating a sub-20 ps resolution. We believe the current system is capable of 10 ps without any major adjustments, and are working on some minor refinements. There is still R&D in progress on several fronts, as outlined below, although no one in AFP is currently working on the GASTOF detector.

5.6.1 Detector R&D

The detector development effort to date has demonstrated that fused silica bars produce enough light within a reasonable time range to meet our detector resolution goals. Prototype tests have generally been one row (8 channels), while the final detector design needs to be refined to incorporate all the channels, and offset the two detectors to reduce the bin size and avoid "cracks" (regions of poor acceptance). We have preliminary indications that a low pass filter is somewhat beneficial to the overall resolution–less light implies worse resolution, but a narrower color range would reduce the resolution broadening from color dispersion.

Another development issue is reducing the size of detector bins close to the beam, while maintaining the same MCP-PMT pixel size to equalize the rate per unit area. Not only would this improve the multi-proton timing capability (which becomes important at high luminosity, where the overlap background is worst), but it would also reduce the rate and lifetime requirements of the MCP-PMT, which are dominated by the pixels closest to the beam. Variable detector bin size could be achieved most easily with quartz fibers instead of quartz bars, and such an option is being explored by Giessen, but can also be done using quartz bars connected to fibers or channeling the light with short air light guides or Winston cones.

5.6.2 MCP-PMT R&D

A key issue is the degradation of the quantum efficiency of the MCP-PMT photocathode from back-scattered positive ions. We have estimated that at high luminosity the hottest pixels of the MCP-PMT's would receive 10 to 20 C/cm^2, which would render them unusable on a few week

time scale, so development of an MCP-PMT with a 20 to 30 times longer life is essential. The standard approach to improving the lifetime is to add an ion barrier, a thin film that inhibits the flow of positive ions. The ion barrier method, originally developed for use in night vision devices [52], has been adapted for MCP-PMT's and has been observed to give at least a factor of five lifetime improvement [53]. Recent results with the Hamamatsu SL10 indicate that the lifetime is stable to several C/cm^2 which could already be acceptable for Stage 1.

UTA is working on a Small Business proposal with Arradiance and Photonis, incorporating atomic layer deposition (ALD) coated MCP's into the Photonis Planacon, and evaluating the lifetime. Initial results are very promising, and this approach could be used in conjunction with an ion barrier to provide the life time improvement required for Stage 2. We are also involved with Photek, another MCP-PMT vendor that is interested in making long life MCP-PMT's using a more robust "solar blind" photocathode, and could combine this with the other lifetime improvements into an Ultra long life MCP-PMT.

5.6.3 Electronics R&D

We have developed and tested a prototype of the full electronics chain, but some R&D is still in progress. We are developing an amplifier PCB board to replace the discrete components, and the trigger circuit must be validated. The location of the detectors close to the beam pipe but far from the ATLAS IP, requires moderately radiation-hard electronics on-detector. The location at 220 m from the ATLAS IP has expected radiation levels around 2 10^{11} neutron-equivalent per cm^2 at the beam pipe (this corresponds to a luminosity of 100 fb^{-1}, or 10^7 at an instantaneous luminosity of 10^{34} cm^{-2} s^{-1}) decreasing with distance. At the position of the MCP-PMT and the pre-amplifier, the levels are expected to be 10^{10} or less. This leads to an integrated dose on the order of $\sim$ 200 Grays for a luminoisty of 100 fb^{-1}. We expect to install the remainder of the timing electronics will in the alcove at 240 m, where the expected dose is of the order of 0.1 to 1 Gray). We plan to analyze radiation monitoring data as the luminosity increases, to develop a more thorough understanding of the radiation environment of the detector. We then plan radiation studies of the quartz bars or fibers, the amplifier board, and the MCP-PMT itself. With a lower priority we will irradiate the remote electronics as well. components as well, but note that all other electronics are located away The mechanics, grounding, and shielding will have to be studied in detail based on the final choice of MCP-PMT. We also must conduct further studies to minimize the effect of the coax signal cable runs on the timing resolution and jitter.

The existing Constant Fraction Discriminator (ALCFD) works well, but it would be beneficial to have programmable gain (or adjustable attenuation) for optimal CFD performance. We will also explore the feasibility of adding a low resolution 8 bit ADC for monitoring the MCP-PMT gain, and perhaps correcting for small or pathological pulses. We plan to route the fast timing signals to the motherboard where the fast trigger circuitry will be implemented. The fast signals, the reference time signal, and the row trigger signal will be transmitted via the analog backplane to the time digitizer modules. A dedicated VME trigger module forms the OR of all row triggers into a single-arm master trigger for transmission to the ATLAS central trigger processor.

When a trigger occurs, the high-precision reference clock signal is passed along with the row signals for digitization. The trigger logic must preserve the channel timing resolution and introduce a channel jitter of less than 5 ps. The trigger logic, although quite straight-forward remains to be designed and implemented.

We have developed and tested a single chip HPTDC board, but will need to redesign it to use 3 HPTDC chips to account for the 80 MHz internal clock as described above, which limits the chip to four useful channels, one of which is dedicated to the clock signal. Minor modifications

are needed to the reference timing circuit developed by SLAC to adapt from the 476 MHz SLAC RF to the 400 MHz LHC RF, and to convert the 400 MHz stabilized clock to 40 MHz and interface it with the trigger board.

We anticipate that the timing front-end electronics will be developed and tested by 2013, if either of two pending U.S. grants to support this development are funded. Without funding, we still expect to be able to develop a working prototype of the entire chain, but would not be able to build the production version. A first prototype of the amplifier board should be ready for test beam this summer. The connection to the ATLAS DAQ chain via the RODs can be achieved within a year. The radiation testing of the front-end amplifier will be carried out within the next year, allowing time for any necessary iteration of the design.

5.7 Timing summary

We are in the process of developing an ultra-fast TOF detector system that will have a key role in the AFP project by helping to reject overlap background that can fake our signal. Tests of the current prototype detector design imply an initial detector resolution of 10 to 15 ps, including the full electronics chain. For a luminosity of $\mathcal{L} \approx 2 \times 10^{33}$ cm^{-2}s^{-1}, a 30 ps detector would be sufficient to keep the overlap background to the level of other backgrounds for the dijet channels, and render it negligible for other final states. For $\mathcal{L} \approx 5 \times 10^{33}$ cm^{-2}s^{-1}, a 10 ps detector (still with loose vertex cuts to maximise signal efficiency) would be desirable to keep overlap backgrounds totally under control, without any loss in signal efficiency. For substantially higher luminosity, we would control the background by improving the timing detector resolution to the 5 ps range and/or tightening the vertex window or other background cuts (a factor of several in rejection is possible with modest lost of efficiency).

The simplest approach to achieving faster timing is minor upgrades to current detector technologies. For the QUARTIC detector a next generation MCP-PMT with smaller pixel sizes would allow finer x segmentation for improved multi-proton timing. A smaller pore size would also be expected to give a modest improvement in the time resolution. Better electronics, such as a second generation HPTDC chip under discussion (5 to 10 ps least bit) could also give an incremental improvement and be beneficial for the GASTOF detector which is electronics-limited. Recent improvements in siPM's are promising (could have a QUARTIC-like design read out by SiPM's which would avoid the radiation hardness questions by keeping the SiPM's away from the main flux of particles). We will continue to follow R&D in this area, as well as monitor advances in other technology for possible upgrades for Stage 2.

Chapter 6

Timescale, Resources, and Conclusions

6.1 Timeline

An overview of major milestones of the AFP Stage I project from now through installation assuming approval:

- *04/2011:* Forward Detector group endorses project, AFP recognized as ATLAS R&D project, AFP group fully integrated in Forward Group
- *7–12/2011:* Development of first silicon prototype and Hamburg pipe prototype, timing detector electronics full chain test with laser
- *end of 2011:* Beam tests of Si and timing detectors
- *2012* AFP recognized as ATLAS upgrade project, finalize R&D, beam test of full system prototype; preparation, submission, and review of TDR
- *beginning of 2013:* Approval of AFP by ATLAS/LHCC and testing of final prototypes
- *2013:* Construction and testing of production detectors, software development
- *1–3/2014:* Installation of 220 m system

A proposal of the timescale for the project is outlined below for the different parts of the project:

- Movable beam pipe
  - *05/2011:* Continue interactions with CMS/LHC Vacuum group on movable beam pipe design
  - *starting Summer 2011:* Safety committee created together with CMS/LHC Vacuum group
  - *beginning 2012:* Construct prototypes of movable beam pipe
  - *mid 2012:* Integrated beam tests with movable beam pipe, QUARTIC, silicon sensors
- Silicon Pixel detectors
  - *Autumn 2011:* First sensors ready - Bump-bonding of first sensors to FEI4 chips by Fraunhofer (Berlin)

- *09/2011:* Cabling of bare modules
- *12/2011:* First detector ready for beam tests, prototype of cooling system
- *end 2011-2012:* Alignment and support studies
- *December 2011:* Prototype of cooling system
- *end 2012:* Production of final detectors

- Timing detectors (see timing chapter for detailed R&D plan)
  - *fall 2011:* Test beam with fiber detector prototype and quartz bar prototype and full electronics chain
  - *2012* Radiation tests and finalize electronics and detector design, PMT development continues, final prototype tests
  - *2013* Tests of production system with final detector and MCP-PMT

6.2 Installation

The proposal is to install the following during the 2013/2014 shutdown:

1. the movable beam pipes located at 216 and 224 m on both sides of the ATLAS detector
2. cables and fibers in tunnel connecting the AFP stations to ATLAS trigger and readout
3. local cables and electronics including LV/HV and reference timing receiver box in alcove near detectors
4. silicon tracking detectors (and cooling) in each of the four stations
5. QUARTIC timing detectors: one in each 224 m station after silicon

If for some reason only a partial system could be installed, it would be desirable to at least complete the first two items, as the last three could in principle be installed during a minor access period. We fully expect to have production timing detectors as well, and at a minimum would plan to install prototypes. The silicon detector timescale depends critically on IBL development. It seems likely that at least some prototypes would be ready for installation, while the final detectors might be delayed until the next winter shutdown. If sufficient manpower and funds were added to the project (motivated by a BSM Higgs discovery in 2011 for example), the proposal could be upgraded to include installation of 420 m detectors as well on the same timescale (or else they would have to wait for the next long shutdown).

Following the recommendations from the referees, we decided to simplify the installation aims for the 2013-14 shutdown as follows:

- **Movable beam pipe:** At 216 m, we will build the movable beam pipe with one pocket which will contain the Si detector, while at 224 m, we will have either a two pocket solution (same short pocket for the silicon plus another shortish pocket for the QUARTIC) or one medium pocket to house both detectors. By fixing the Hamburg pipe length at 50 cm or so, we would have one single Hamburg pipe motion system, and could change pocket length as needed by simply swapping out that section of pipe in a modest length shutdown. Deferring the GASTOF detector will simplify the beam pipe design and avoid the gas flow. This can be upgraded in a next phase of the project if needed (the cost of the movable beam pipe is moderate as shown further in the document)

Institute	Activity	Manpower Total People	Manpower FTE
Armenia	timing detectors	2	1
Czech Republic	Pixel Si detector Cooling	12	5
France, CEA Saclay	Mechanical Engineering Timing detector electronics	10	4
Germany, Giessen	Timing detectors	2	1
Poland	Power supplies	8	4
USA, Texas Arlington	QUARTIC trigger	3	1.5
USA, Stony Brook	QUARTIC	2	1.3
Alberta, Canada	QUARTIC trigger	4	2

Table 6.1: Minimum manpower foreseen to be available through installation if AFP project approved.

- **Silicon detector:** We will follow the IBL decision concerning the type of Si detector to be built (either n-on-n or 3D). This will allow us to benefit from the IBL experience concerning the sensors, tests and software developments and to collaborate with them. If the 3D solution is not chosen, it could be an upgrade of our detector for the 2017-18 shutdown since this is the best detector for us (the edgeless aspect allows to detect protons closer to the beam, the dead zone being smaller)

- **Timing detector:** as we mentioned in the first bullet, we plan to concentrate on QUARTIC detectors only in the first phase of the project and would install one in each 224 m station.

6.3 Personnel

Due to this project's current lack of status within ATLAS, the active manpower is extremely limited. The current effort is primarily limited to timing detector R&D. Approval of the technical proposal would immediately ramp up involvement of several groups as shown in Table 1. Other groups that have expressed interest would also likely join the effort and new groups would be recruited.

The manpower available as well as the activities concerning the Si detector which could be covered by Prague are detailed in Tables 6.3 and 6.3.

6.4 Costing and available or requested budget

A detailled cost for the different parts of the project is given in Tables 6.4, 6.1, 6.4 and 6.4. The total cost for the project is about 1.9 million CHF, to which we need to add the cost of the two collimators to be added if the LHC beam division does not pay for it.

The available and requested budgets per country for the project are given in the following (please note that this is just indicative at this stage of the project):

Task	Planar n-n	3D
Sensor design	IBL	
Sensor production	x	
Sensor lab tests	x	
Flip-chip bonding	IBL	
FE-I4 production	IBL	
Test beams	x	x
Irradiation tests	IBL	x
Module assembly	x	
Installation	x	
DAQ development	x	x
Power supplies	x	x
External services	x	
Off-sensor readout	x	x
Det.Control System	x	x
Cooling	x	x

Table 6.2: Activities which can be performed in Prague in collaboration with the IBL group if the n-on-n or 3D option is chosen.

- **Armenia:** Some money can be requested once project is approved.
- **Canada:** 70 kCHF available now for engineer/technician salaries, additional money can be requested once the project is approved
- **Czech Republic:** Money is available for wafers, FEI4 chips, n-on-p sensors (production, tests, flip-chip bonding), if this solution is chosen, as well as cooling of the Si detector
- **France:** Some funds will be available to develop Stage II fast timing electronics when the AFP project is an ATLAS project; engineers can be committed to the project (salaries paid)
- **Germany:** 50% post-doc for timing detector development now, possibility to submit a funding application to BMBF if project considered as an ATLAS project by the end of this year
- **Poland:** A grant from Polish government can be requested once the project is an ATLAS project and the MoUs are signed
- **USA:** UTA MCP-PMT development project funded ($150,000), Stony Brook Electronics technician funded ($35,000), DOE ADR submitted for timing electronics development ($173,000), other fundinf requests planned if approved.

6.5 Conclusion

This Technical Proposal has presented the Stage I plan of the ATLAS Forward Proton (AFP) upgrade: to add high precision silicon and timing detectors housed in specialized movable beam pipes at $\sim$ 220 m upstream and downstream of the ATLAS interaction point to detect intact final state protons scattered at small angles and with small momentum loss. The detectors would be

Task	# people	time
Sensor design and production	2	4m/2011
Test beams	2	2m/2011-2013
Lab tests	4	2m/2011-2012
Irradiation tests	2	1m/2011-2012
Module assembly	2	1m/2011, 4m/2012
Installation	2	4m/2013
DAQ development	2	6m/2011-2013
Power supplies	1	1m/2011-2013
External services	1	1m/2011-2013
Off-sensor readout	1	1m/2011-2013
Det.Control System	1	1m/2011-2013

Table 6.3: Manpower (person month) available for the pure AFP part of the Si detector in case the n-on-n solution is chosen. Much more manpower from Prague is devoted to the IBL project benefitting directly to AFP since we will follow the recommendations from the IBL group.

element	unit cost	total cost
Single/double pocket pipe, flanges, SV box	15	60
Tables	7	28
Bellow units	4.5	36
BPMs	10	120
Movement system (with mechanics)	80	320
Vacuum pump (secondary vacuum)	2	6
Total		**570**

Table 6.4: Cost of the movable beam pipes (in kCHF).

fully integrated into ATLAS forming a new proton detection capability during standard running thus enabling a rich QCD, electroweak and beyond the Standard Model experimental program. For this project to succeed, it must rapidly be declared an ATLAS upgrade project, enabling funding for the final R&D needed for the Technical Design Report. Given final ATLAS/LHCC approval by late 2012 and the procurement of sufficient funds it would be possible to install the full 220 m system in early 2014. Finally, we would like to acknowledge the tremendous work done by the UK groups which initiated this project and sadly have been forced by their funding agencies to abandon it.

Item	Minimal System Number	Full System Number	Unit Cost	Minimal Cost	Full Cost	Spare Cost	Min Spare Cost	Min Cost w/spares	Full Cost w/Spares
Detectors									
QUARTIC	2	4	$7,000	$14,000	$28,000	$14,000	$14,000	$28,000	$42,000
QUARTIC PMT	2	4	$20,000	$40,000	$80,000	$40,000	$40,000	$80,000	$120,000
GASTOF		2	$8,000	$0	$16,000	$8,000		$0	$24,000
GASTOF PMT		2	$24,000	$0	$48,000	$24,000		$0	$72,000
Gas System		2	$14,000	$0	$28,000	$2,000		$0	$30,000
Detector Cost				**$54,000**	**$200,000**	**$88,000**	**$54,000**	**$108,000**	**$288,000**
Electronics									
8-ch Preamps	8	18	$400	$3,200	$7,200	$800	$800	$4,000	$8,000
8-ch CFD	8	18	$3,400	$27,200	$61,200	$6,800	$6,800	$34,000	$68,000
HPTDC	8	16	$3,450	$27,600	$55,200	$6,900	$6,900	$34,500	$62,100
8-ch ADC	10	18	$128	$1,280	$2,304	$256	$256	$1,536	$2,560
Trigger Logic	2	2	$2,500	$5,000	$5,000	$2,500	$2,500	$7,500	$7,500
Calibration Pulser	2	2	$3,600	$7,200	$7,200	$3,600	$3,600	$10,800	$10,800
Reference clock	2	2	$17,150	$34,300	$34,300	$17,150	$17,150	$51,450	$51,450
Electronics Cost				**$105,780**	**$172,404**	**$38,006**	**$38,006**	**$143,786**	**$210,410**
Cables									
Clock Cables	2	2	$7,800	$15,600	$15,600	$15,600	$15,600	$31,200	$31,200
Trigger Cables	2	2	$7,800	$15,600	$15,600	$15,600	$15,600	$31,200	$31,200
HV cables			$5,000	$5,000	$5,000	$500	$500	$5,500	$5,500
Low Voltage Cables			$5,000	$5,000	$5,000	$500	$500	$5,500	$5,500
Other Cables			$10,000	$10,000	$10,000	$1,000	$1,000	$11,000	$11,000
Fibers			$5,000	$5,000	$5,000	$500	$500	$5,500	$5,500
Cable Cost				**$56,200**	**$56,200**	**$33,700**	**$33,700**	**$89,900**	**$89,900**
Infrastructure									
HV	2	2	$10,000	$20,000	$20,000	$10,000	$10,000	$30,000	$30,000
LV	2	2	$5,000	$10,000	$10,000	$5,000	$5,000	$15,000	$15,000
VME-type crates with PS	2	2	$7,500	$15,000	$15,000			$15,000	$15,000
VME-ROD controller	2	2	$5,000	$5,000	$5,000			$5,000	$5,000
ROD	2	2	$6,000	$5,000	$5,000			$5,000	$5,000
TTC Modules	2	2	$5,000	$10,000	$10,000			$10,000	$10,000
Infra cost				**$65,000**	**$65,000**	**$15,000**	**$15,000**	**$80,000**	**$80,000**
TOTAL COST				**$280,980**	**$493,604**	**$174,706**	**$140,706**	**$421,686**	**$668,310**

Figure 6.1: Costs for the timing detectors. The number in red are not yet precisely known.

50 chips/5 wafers	**Planar n-n**	**3D**
masks	11.5	
wafers	0.7	
processing	6.4	
testing	0.5	
Total	**19.1**	**30.8**

Table 6.5: Cost of the chips and wafers for the n-on-n and 3D options.

System	Item	Description	Cost (kCHF)	
			IBL	AFP220
Module	1	Sensor - prototype, production, procurement & QC	752	15
	2	FE-I4 prototype, production, test	1372	100
	3	Bump-bonding, thinning, bare module -prototype, prod. & QC	726	100
Stave	4	Local support: CF structure, TM, pipe-prototype, prod. & QC	467	46.7
	5	Module assembly, stave loading, flex-hybrid, internal electrical services - design, prod. & QC	436	43.6
Off-detector	6	R/O chain: opto-board, opto-fiber, TX/RX, BOC, ROD, TDAQ (S-link, TIM, SBC, ROS, crate)	1025	102.5
	7	Power chain: HV/LV PS, PP2 regulators, type 2, 3 & 4 cables, interlocks, DCS	505	50.5
Integration	8	Integration in SR1 & System test	492	49.2
Cooling plant	9	Cooling plant & cooling services to PP1	461	100
		Total	**6236**	**608**

Table 6.6: Costs of the Si detector for IBL and AFP.